Concentrations and origins of atmospheric lead and other trace species at a rural site in northern China

Can Li,[1,2] Tianxue Wen,[3] Zhanqing Li,[1,3,4] Russell R. Dickerson,[4] Yongjie Yang,[5] Yanan Zhao,[3] Yuesi Wang,[3] and Si-Chee Tsay[2]

Received 1 December 2009; revised 30 June 2010; accepted 7 July 2010; published 15 October 2010.

[1] In this study we analyze the ambient levels of lead and other trace species in the bulk aerosol samples from a rural site ~70 km ESE of Beijing in spring 2005. Lead (0.28 ± 0.24 μg/m^3, average ± standard deviation), along with several pollution-related trace elements, was enriched by over 100 fold relative to the Earth's crust. The ambient lead levels showing large synoptic variations were well-correlated with other anthropogenic pollutants (e.g., CO and SO_2). The Unmix receptor model resolved four factors in the aerosol composition data: a biomass burning source, an industrial and coal combustion source, a secondary aerosol source, and a dust source. The first three sources were strongest in weak southerly winds ahead of cold fronts, while the dust source peaked in strong northerly winds behind cold fronts. The second source, primarily representing emissions from industrial processes and relatively small-scale coal burning such as in home and institutional heating, was identified as the main source of ambient lead in this study. Mobile sources might also contribute to this factor, but there was no distinct evidence of emissions due to combustion of leaded gasoline, despite a correlation between lead and CO. Potential source contribution function, calculated from backward trajectories and aerosol composition, further reveals that lead observed in this study was predominantly from the populated and industrialized areas to the south and SW of Xianghe, rather than Beijing to the west. Our results and several recent studies show that the lead levels in suburban areas near big cities in China, although generally lower than those in industrial districts and urban areas, are substantial (near or above 0.15 μg/m^3). More extensive studies on airborne lead and its emission sources in China are called for.

Citation: Li, C., T. Wen, Z. Li, R. R. Dickerson, Y. Yang, Y. Zhao, Y. Wang, and S.-C. Tsay (2010), Concentrations and origins of atmospheric lead and other trace species at a rural site in northern China, *J. Geophys. Res.*, *115*, D00K23, doi:10.1029/2009JD013639.

1. Introduction

[2] Lead (Pb), widely produced and utilized by humans for thousands of years, is also well known for its adverse health effects [*U.S. Environmental Protection Agency* (*U.S. EPA*), 2006]. Controlling measures such as the phase out of leaded gasoline have been effective in reducing ambient lead [e.g., *U.S. EPA*, 2007a]. The negative effects of Pb on the environment are, however, long-lasting: historically emitted Pb having contaminated soil through wet and dry deposition can reenter the atmosphere as surface soil is disturbed by wind or other mechanical processes. This has been identified as an important source of ambient Pb in different areas in the United States [e.g., *Ehrman et al.*, 1992; *Harris and Davidson*, 2005], along with industrial processes (e.g., lead smelting, lead-acid batteries), transportation (e.g., wear of on-road vehicles, aircraft and off-road vehicles using leaded fuels), combustion (e.g., utility boilers), and waste management (e.g., incinerators) [*U.S. EPA*, 2007a]. Even at relatively low exposure levels, Pb can still cause health problems for both children and adults. This results in the adjustment of the U.S. ambient standard for lead to 0.15 μg/m^3 on a 3 month rolling basis [*U.S. EPA*, 2006].

[3] In China, a fast emerging economic power and the most populous country of the world, lead pollution has also raised growing concerns in recent years. The phase out of leaded gasoline in China took place in 2000, with the few biggest cities (Beijing, Shanghai, Guangzhou, and Tianjin) taking actions a few years earlier [*Sun et al.*, 2006]. The

[1]Earth System Science Interdisciplinary Center, University of Maryland, College Park, Maryland, USA.
[2]NASA Goddard Space Flight Center, Greenbelt, Maryland, USA.
[3]Institute of Atmospheric Physics, Chinese Academy of Sciences, Beijing, China.
[4]Department of Atmospheric and Oceanic Science, University of Maryland, College Park, Maryland, USA.
[5]National Research Center for Environmental Analysis and Measurement, Beijing, China.

Copyright 2010 by the American Geophysical Union.
0148-0227/10/2009JD013639

ambient levels of lead since the banning of leaded gasoline, reported by several studies mainly conducted in the eastern part of China [e.g., *Chen et al.*, 2008; *Lv et al.*, 2006; *Sun et al.*, 2004, 2006; *Ye et al.*, 2003; *Zhang et al.*, 2005], range from ~0.05 $\mu g/m^3$ in rural areas to ~0.5 $\mu g/m^3$ in more industrialized regions. While generally in accordance with the National Ambient Air Quality Standards of China (1.5 $\mu g/m^3$ for quarterly average, 1 $\mu g/m^3$ for annual average) [*China Ministry of Environmental Protection*, 1996], the reported concentrations are often well above the new U.S. standard. Elevated blood lead levels, which have been associated with deficits in IQ, neurobehavioral development, and physical growth in young children [e.g., *Shen et al.*, 2001], were found to be pervasive, particularly among children in cities [e.g., *Shen et al.*, 1996, 2001; *Wang and Zhang*, 2006] and areas engaged in electronic waste recycling [e.g., *Huo et al.*, 2007]. The lead emission sources in China remain largely uncharacterized. Measurements of lead isotopes in cities [e.g., *Chen et al.*, 2005; *W. Wang et al.*, 2006], and sampling of vehicle exhaust [e.g., *Bi et al.*, 2007], in general, show that leaded gasoline is no longer the major lead source in China. *Li et al.* [2009] notice that lead in Shanghai after the phase out of leaded fuel shows some evidence for a decreasing trend from 2002 to 2006. They maintain that residual Pb in unleaded fuel still accounts for half or more of the atmospheric lead. Several receptor modeling studies, on the other hand, attribute the ambient lead in China to coal burning, industrial processes, and resuspension of previously deposited lead [e.g., *Bi et al.*, 2007; *Lv et al.*, 2006; *Sun et al.*, 2006]. Using single particle mass spectrometry, *Y. Zhang et al.* [2009] conclude that 45% of the Pb-rich particles could be attributed to coal combustion. Other important sources include waste incineration, the phosphate industry, and particles from metallurgical processes.

[4] In this study, we present chemical composition data from the bulk (total suspended particulate, TSP, all liquid or solid particles suspended in the atmosphere) aerosol samples collected in Xianghe, a rural site about 70 km ESE of Beijing in spring 2005, during the ground field campaign of EAST-AIRE (East Asian Study of Tropospheric Aerosols: An International Regional Experiment) [*C. Li et al.*, 2007]. We focus in particular on lead in the aerosol samples, discussing its abundance, synoptic variation, and correlation with other elements. We also use a receptor model to identify the main sources of aerosols, and derive their contributions to ambient lead levels. Backward trajectories are then employed to determine the potential source regions for lead. This is followed by a review of several recent studies about airborne lead and aerosol composition in China.

2. Methodology

2.1. Aerosol Sampling

[5] During the experiment, a high-volume aerosol sampler collected particles (no size cut) on Whatman 41 quantitative filter paper (8 by 10 in, or 20.32 by 25.4 cm), at about 15 m above ground. A manometer measures the pressure drop as the sampling flow passes through a critical orifice. The recorded pressure drop was used to calculate the flow rate, which starts at about 800 L/min initially upon filter change and drops as the filter becomes loaded with particles. Depending on aerosol loading, the total volume of air sampled by each filter ranges from 400 to 500 m^3 during the 12 h sampling period (0800–2000 local time (LT) for daytime samples and 2000–0800 LT for nighttime samples). From 2 March to 13 April, 83 samples were collected along with blank samples taken every 10 days. Both exposed and blank filters were stored in a freezer until chemical analysis.

[6] The sampling site, Xianghe (39.798°N, 116.958°E, 35 m above sea level), is one of the super sites of EAST-AIRE aerosol observation network, and has been described in detail elsewhere [*Z. Li et al.*, 2007, also Overview of the East Asian Study of Tropospheric Aerosols and Impact on Regional Climate (EAST-AIRC), submitted to Journal of Geophysical Research, 2010]. It is located in a small village with some local emission sources (e.g., residence, small boilers, and small factories), but only 5 km west of the local township (population: ~ 50,000), and 70 km ESE of Beijing, a mega city with more than 13 million residents. Throughout the experiment, it was generally cold (average temperature ~ 8°C) and dry (average relative humidity (RH) ~ 38%), and seldom rained [*C. Li et al.*, 2007].

2.2. Chemical Analysis

[7] The chemical analysis of the aerosol samplers was conducted at the Institute of Atmospheric Physics (IAP), Chinese Academy of Sciences (CAS), and is briefly described here. For elemental analysis, one eighth of the filters were first digested in concentrated AR grade HNO_3 (6 mL) and HCl (2 mL) for 40 min, using a microwave sample digestion system (PerkinElmer Life and Analytical Sciences, Inc., Model Multiwave 3000, Waltham, Massachusetts). The digestion process is based on U.S. EPA method 3052, and the recovery rate for various elements has been determined with standard soil and fly ash samples (GBW07401 and GBW08401) certified by the Administration of Quality Assurance, Inspection, and Quarantine of China (AQSIQ). The recovery rate for Al from the certified samples is ~50%, and a correcting factor of 2 is applied to the Al concentration. An inductively coupled plasma mass spectrometer (ICP-MS, Agilent Technologies, Inc., Model 7500a, Santa Clara, California) was used to analyze elements including Be, Na, Mg, Al, K, Ca, V, Mn, Fe, Ni, Cu, Zn, As, Mo, Ag, Cd, Ba, Tl, Pb, Th, and U. Calibration with reference material (Environmental Calibration Standard, Part 5183–4688, Agilent Technologies) demonstrates good linearity and sensitivity of the instrument. The relative standard deviation for each measurement (repeated three times) is within 3%. The detection limits determined through analyses of blank samples are better than 2 ng/m^3 for all elements.

[8] One eighth of each filter was ultrasonically extracted in 50 mL deionized water (resistivity: 18 MΩ/cm) for about 30 min. The filtrate, after passing through a microporous membrane (0.45 μm in pore size), was then analyzed with an ion chromatograph (IC, Dionex Corporation, Model ICS-90, Sunnyvale, CA) for the concentrations of F^-, Cl^-, NO_3^-, SO_4^{2-}, NH_4^+, Ca^{2+}, Na^+, Mg^{2+}, and K^+. The IC was periodically checked with standard reference materials (Merco Co.), and the ion recovery was ~80–120%. The relative standard deviation for each measurement (repeated three times) is controlled within 3%. All

Table 1. Statistics of Water-Soluble Inorganic Ions and Elements in Bulk Aerosol Samples From Xianghe ($\mu g/m^3$)

Element	Mean	Standard Deviation	Median	10th Percentile	25th Percentile	75th Percentile	90th Percentile
F^-	1.4×10^{-1}	1.2×10^{-1}	1.1×10^{-1}	1.2×10^{-2}	2.8×10^{-2}	2.2×10^{-1}	3.4×10^{-1}
Cl^-	3.4	2.7	3.2	6.4×10^{-1}	1.1	4.6	6.4
NO_3^-	9.5	9.3	6.4	9.1×10^{-1}	2.1	13.0	21.1
SO_4^{2-}	7.1	6.3	5.0	1.7	2.7	8.9	14.3
Na^+	6.6×10^{-1}	3.8×10^{-1}	6.3×10^{-1}	2.2×10^{-1}	4.1×10^{-1}	8.7×10^{-1}	1.1
NH_4^+	5.4	4.3	4.4	1.1	1.8	7.3	11.5
K^+	1.4	1.0	1.1	3.4×10^{-1}	6.0×10^{-1}	2.0	3.1
Ca^{2+}	3.4	1.6	3.2	1.3	2.3	4.6	5.3
Mg^{2+}	3.0×10^{-1}	1.5×10^{-1}	2.8×10^{-1}	1.2×10^{-1}	1.8×10^{-1}	3.9×10^{-1}	4.8×10^{-1}
Be	3.9×10^{-4}	1.7×10^{-4}	3.6×10^{-4}	1.8×10^{-4}	2.6×10^{-4}	4.8×10^{-4}	6.4×10^{-4}
Na	1.2	5.7×10^{-1}	1.2	4.5×10^{-1}	8.2×10^{-1}	1.6	2.0
Mg	3.1	1.6	2.7	1.2	2.2	4.0	5.0
Al	9.8	5.3	8.4	3.6	6.3	11.9	15.5
K	3.6	2.0	3.1	1.2	2.0	5.1	6.6
Ca	10.0	4.7	9.5	3.5	6.6	13.6	16.2
V	1.2×10^{-2}	6.4×10^{-3}	1.1×10^{-2}	3.9×10^{-3}	6.8×10^{-3}	1.6×10^{-2}	2.0×10^{-2}
Mn	1.7×10^{-1}	8.3×10^{-2}	1.7×10^{-1}	5.8×10^{-2}	1.1×10^{-1}	2.2×10^{-1}	2.8×10^{-1}
Fe	6.6	3.4	6.0	2.1	4.2	8.9	11.4
Ni	1.2×10^{-2}	3.6×10^{-2}	7.3×10^{-3}	3.2×10^{-3}	4.8×10^{-3}	1.1×10^{-2}	1.6×10^{-2}
Cu	7.6×10^{-2}	1.6×10^{-1}	3.0×10^{-2}	6.4×10^{-3}	1.3×10^{-2}	7.7×10^{-2}	1.7×10^{-1}
Zn	4.4×10^{-1}	3.7×10^{-1}	3.9×10^{-1}	4.5×10^{-2}	8.6×10^{-2}	6.3×10^{-1}	9.0×10^{-1}
As	1.8×10^{-2}	1.4×10^{-2}	1.4×10^{-2}	3.1×10^{-3}	5.4×10^{-3}	2.6×10^{-2}	3.6×10^{-2}
Mo	2.7×10^{-3}	2.1×10^{-3}	2.2×10^{-3}	4.5×10^{-4}	9.2×10^{-4}	4.0×10^{-3}	5.3×10^{-3}
Ag	5.9×10^{-4}	4.9×10^{-4}	5.6×10^{-4}	6.6×10^{-5}	1.6×10^{-4}	8.4×10^{-4}	1.2×10^{-3}
Cd	4.5×10^{-3}	3.8×10^{-3}	3.6×10^{-3}	4.3×10^{-4}	8.1×10^{-4}	6.6×10^{-3}	9.6×10^{-3}
Ba	9.3×10^{-2}	5.3×10^{-2}	7.9×10^{-2}	3.7×10^{-2}	5.8×10^{-2}	1.1×10^{-1}	1.8×10^{-1}
Tl	2.2×10^{-3}	2.1×10^{-3}	1.6×10^{-3}	3.1×10^{-4}	5.9×10^{-4}	3.3×10^{-3}	4.6×10^{-3}
Pb	2.8×10^{-1}	2.4×10^{-1}	2.1×10^{-1}	2.8×10^{-2}	5.4×10^{-2}	4.5×10^{-1}	6.6×10^{-1}
Th	1.5×10^{-3}	7.6×10^{-4}	1.4×10^{-3}	5.4×10^{-4}	9.0×10^{-4}	1.8×10^{-3}	2.4×10^{-3}
U	4.5×10^{-4}	2.2×10^{-4}	4.2×10^{-4}	1.9×10^{-4}	2.9×10^{-4}	6.0×10^{-4}	7.7×10^{-4}

ions have detection limits below 0.02 $\mu g/m^3$. Quality control and quality assurance procedures were routinely applied for both elemental and ion analyses. More detailed descriptions are available in other studies employing similar analysis system [*Xu et al.*, 2007a, 2007b; *Yang et al.*, 2009].

2.3. Trace Gases and Meteorology

[9] Measurements of trace gases were carried out at the same site from 2 to 26 March 2005 [*C. Li et al.*, 2007]. SO_2 was measured using a modified [*Luke*, 1997] commercial pulsed-fluorescence detector (Thermo Environmental Instruments, TEI Model 43C, Franklin, MA). CO concentration was determined with a modified [*Dickerson and Delany*, 1988] commercial (TEI Model 48, Franklin, MA) analyzer. All trace gas analyzers were calibrated with National Institute of Standards and Technology (NIST) traceable working standards before and after the field campaign. Temperature, relative humidity (RH), wind direction, wind speed, and ambient pressure were monitored with a nearby 32 m meteorology tower.

2.4. Unmix Receptor Model

[10] One commonly applied receptor modeling approach, chemical mass balance (CMB), requires a priori knowledge of the number of sources and source profiles, largely unknown for our study area. Instead we employed the EPA Unmix 6.0 model [*U.S. EPA*, 2007b] to carry out a factor analysis to estimate the number of factors in the chemical composition data, as well as their contributions to different species. Unmix first determines the most probable number of factors (s) in the data matrix, using an approach known as "NUMFACT" [*Henry et al.*, 1999]. The dimensionality of the data is then reduced to s through singular value decomposition (SVD). Further reduction in the data dimensionality is achieved by projecting the data to a plane perpendicular to the principle axis of the s-dimensional space. Unmix then characterizes the edges of the projected data to derive source profiles, which are then used to estimate the source contributions by these factors or sources. In addition, Unmix poses nonnegativity constraints on both source profiles and source contributions, although small negative values are allowed to account for analysis errors [*Henry*, 1997]. Similar to other factor analysis methods (e.g., principle component analysis, positive matrix factorization), Unmix generally requires a sizable data set. The number of samples in this study meets the Unmix recommended lower limit for sample size [*U.S. EPA*, 2007b], and is comparable to a few previous studies also applying the Unmix model [e.g., *Larsen and Baker*, 2003; *Hu et al.*, 2006]. Several other studies used Unmix to analyze larger data sets [e.g., *Chen et al.*, 2002; *Lewis et al.*, 2003].

2.5. Backward Trajectories and Potential Source Contribution Function

[11] We used National Center for Environmental Prediction (NCEP) global reanalysis data with one degree resolution and NOAA Air Resource Lab (ARL) HYSPLIT back-trajectory model (R. R. Draxler and G. D. Rolph, HYSPLIT (HYbrid Single-Particle Lagrangian Integrated

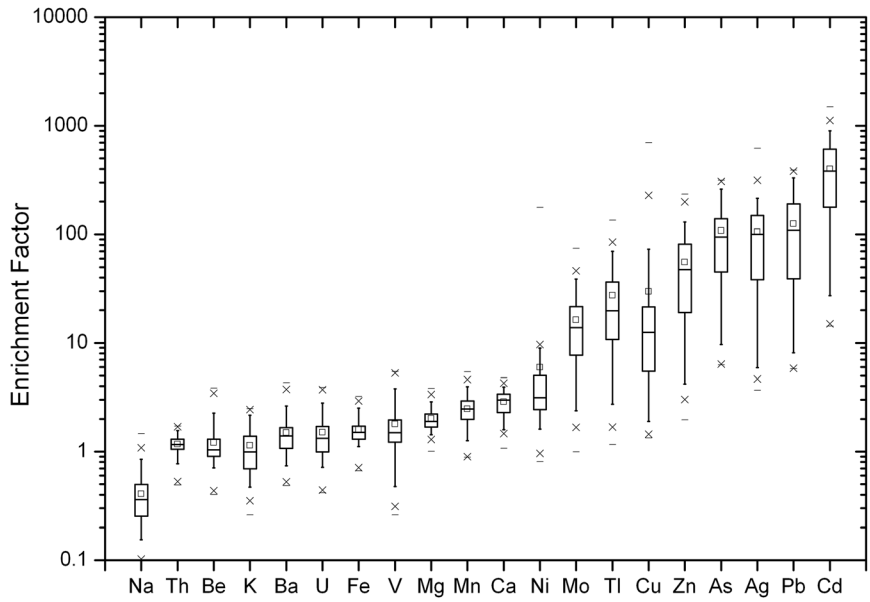

Figure 1. Box and whisker chart of the enrichment factors. The center horizontal line, lower edge, and upper edge of the box represent the median, 25th percentiles, and 75th percentiles, respectively. Lower and upper whiskers are the 10th and 90th percentiles. Crosses stand for the 1st (lower) and 99th (upper) percentiles. Maximum (upper) and minimum (lower) EFs are marked with horizontal lines outside the box body. Squares represent mean EFs. Al is the reference element and not shown in the chart.

Trajectory) Model, 2003, htttp://www.arl.noaa.gov/ready/hysplit4.html) to calculate backward trajectories. For a given aerosol sample, 72 h backward trajectory was initiated at 0200 LT (nighttime sample) or 1400 LT (daytime sample), from 200 m (nighttime sample) or 500 m (daytime sample) above ground level over Xianghe. The trajectory starting heights were selected to represent the diurnal cycle in the thickness of the boundary layer.

[12] Potential source contribution function (PSCF), calculated from backward trajectories in conjunction with chemical composition data, has been widely used to determine of the source regions of pollutants [e.g., *Begum et al.*, 2005; *Zhang et al.*, 2005]. PSCF for the ij^{th} grid cell in a region with $i \times j$ grid cells is defined as

$$PSCF_{ij} = {m_{ij}}/{n_{ij}}, \quad (1)$$

where n_{ij} is the total number of trajectory segment endpoints (i.e., the position of the air parcel at a given time) that fall within the ij^{th} grid cell, m_{ij} is the number of trajectory endpoints in the same grid cell that are associated with samples having pollutant concentrations above an arbitrary criterion. To minimize the artifact due to small n_{ij} values (grid cells with few trajectory endpoints), the $PSFC_{ij}$ is weighted with w_{ij}. A function of n_{ij}, w_{ij} in this study was set at 1 for $n_{ij} \geq 4$, 0.85 for $n_{ij} = 3$, 0.65 for $n_{ij} = 2$, and 0.5 for $n_{ij} = 1$, following *Lucey et al.* [2001].

[13] In this study, we calculated the PSCF based on the distribution of 3 h backward trajectory endpoints over a domain of 1 × 1° grid cells covering the eastern part of China (25°N–50°N, 90°E–130°E). Three different criteria for aerosol composition were applied to determine m_{ij}, namely Pb concentration ($\geq$ 0.4 μg/m^3), Pb enrichment factor (EF) (EF $\geq$ 125), and the strength of the factor contributing the most Pb ($\geq$ 1 unit of the corresponding factor) as estimated with Unmix.

3. Results

3.1. Abundance of Major Inorganic Ions and Elements

[14] The statistics of water-soluble ions (Table 1) show fairly high concentrations of mainly secondary aerosol species such as sulfate (SO_4^{2-}, 7.1 ± 6.3 μg/m^3), nitrate (NO_3^-, 9.5 ± 9.3 μg/m^3), and ammonium (NH_4^+, 5.4 ± 4.3 μg/m^3). Most interestingly, in contrast to a number of previous studies in northern China, our observed NO_3^- mass concentration ([NO_3^-]) is higher than that of SO_4^{2-} ([SO_4^{2-}]). Note that ammonium balances the sum of sulfate and nitrate anion strength (Table 1), and the aerosols are on average alkaline. As a result, vapor HNO_3 is likely collected to the bulk aerosol samples. Loss of ammonium nitrate from the filter paper may also influence the measured nitrate concentration, as backup filters were not used in this study. The [NO_3^-]/[SO_4^{2-}] ratio in Xianghe and its synoptic change will be discussed elsewhere. For comparison, *Chen et al.* [2002] found on average 3.3 μg/m^3 of SO_4^{2-}, 4.1 μg/m^3 of total nitrate (HNO_3 + all particulate NO_3^-) and 1.92 μg/m^3 of total ammonium (NH_3 + particulate NH_4^+) in April fine particle samples collected at a traffic-influenced site in Fort Meade, Maryland.

[15] Table 1 also summarizes the statistics of element concentrations for aerosol samples from Xianghe. High

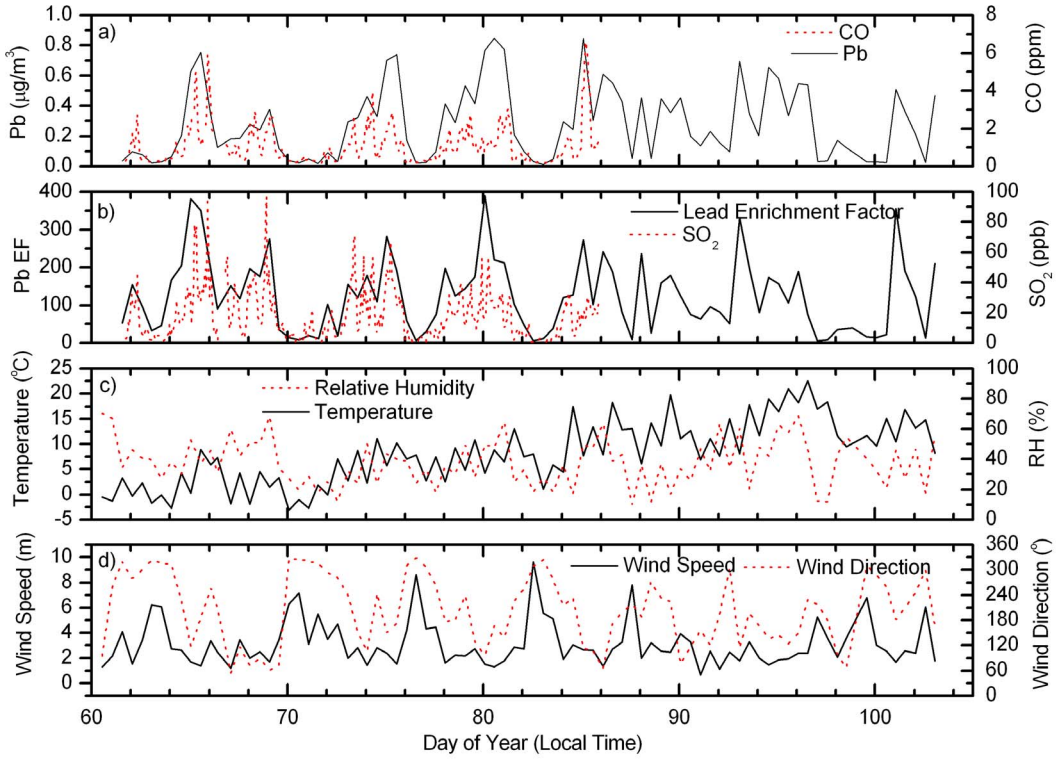

Figure 2. (a) Time series of Pb and CO concentration ($R^2 = 0.50$), (b) enrichment factor of Pb and SO_2 concentration, (c) temperature and relative humidity, and (d) wind direction and wind speed in Xianghe during the experiment in spring 2005.

loadings of crustal elements including Al (9.8 ± 5.3 $\mu g/m^3$), Mg (3.1 ± 1.6 $\mu g/m^3$), Ca (10.0 ± 4.7 $\mu g/m^3$), and Fe (6.6 ± 3.4 $\mu g/m^3$) indicate the existence of soil particles in springtime over the region. Aerosol samples collected at various urban and rural locations in Asia including Japan, Vietnam, Indonesia, Taiwan, and Korea, yielded aerosol Fe concentration of ~0.2–3 $\mu g/m^3$, although Fe levels exceeding 100 $\mu g/m^3$ were recorded for suspended particulate matter at heavily polluted traffic sites in India [*Fang et al.*, 2005 and references therein]. For this non-urban site, the loadings of some pollutant trace elements are also relatively high, in some cases comparable to urban or traffic sites in Asia (e.g., Pb: 0.28 $\mu g/m^3$ versus 0.04–0.34 $\mu g/m^3$; Cu: 76 ng/m^3 versus 20–240 ng/m^3; Zn: 0.44 $\mu g/m^3$ versus 0.12–1.06 $\mu g/m^3$, latter concentration figures from *Fang et al.* [2005] and references therein). The average lead concentration exceeds the newly adapted U.S. ambient standard for lead (section 1), but is below the Chinese standard. The ratio between the 90th percentile and the 10th percentile of each element reflects its variability. Crustal elements in general have ratios between 3 and 5, but the ratios of some pollutant trace elements (e.g., Cu, Ag, As, and Pb) exceed 10, showing large variation in their loadings. Water soluble ions such as sulfate, nitrate, and ammonium, as well as traces gases including CO, SO_2 and NO_y [*C. Li et al.*, 2007] are also found to be very variable. Aerosol optical thickness (AOT) at the same site fluctuated over a wide range of 0.2–4 during the experiment [*C. Li et al.*, 2007].

3.2. Enrichment Factors

[16] Using Al as the reference element, the enrichment factor of an element X in aerosols can be calculated with the following equation:

$$EF_X = \left(\frac{X}{Al}\right)_{Aerosol} \Big/ \left(\frac{X}{Al}\right)_{Crust}, \qquad (2)$$

where $\left(\frac{X}{Al}\right)_{Aerosol}$ is the mass ratio between X and Al in aerosols, while $\left(\frac{X}{Al}\right)_{Crust}$ is the same ratio in the crustal material, taken from *Lide* [1998]. The concentrations of elements in different types of soil vary, but normally by less than a factor of 5 [e.g., *Chen et al.*, 1991]. Take K as an example, the crust K/Al ratio used in this calculation is 0.35, and the same ratio ranges from 0.29 to 0.42 for surface soil of the Gobi deserts [*Xuan*, 2005]. Additionally, our sample digestion method without using HF may not recover all aluminum in aerosol samples, as discussed in section 2.2. The EFs therefore should be interpreted qualitatively rather than quantitatively. If EF_x is close to 1, X in aerosols mainly comes from soil sources. On the other hand if EF_x is much higher than unity, X in aerosols may have important sources other than soil particles. Elements with high EF have been

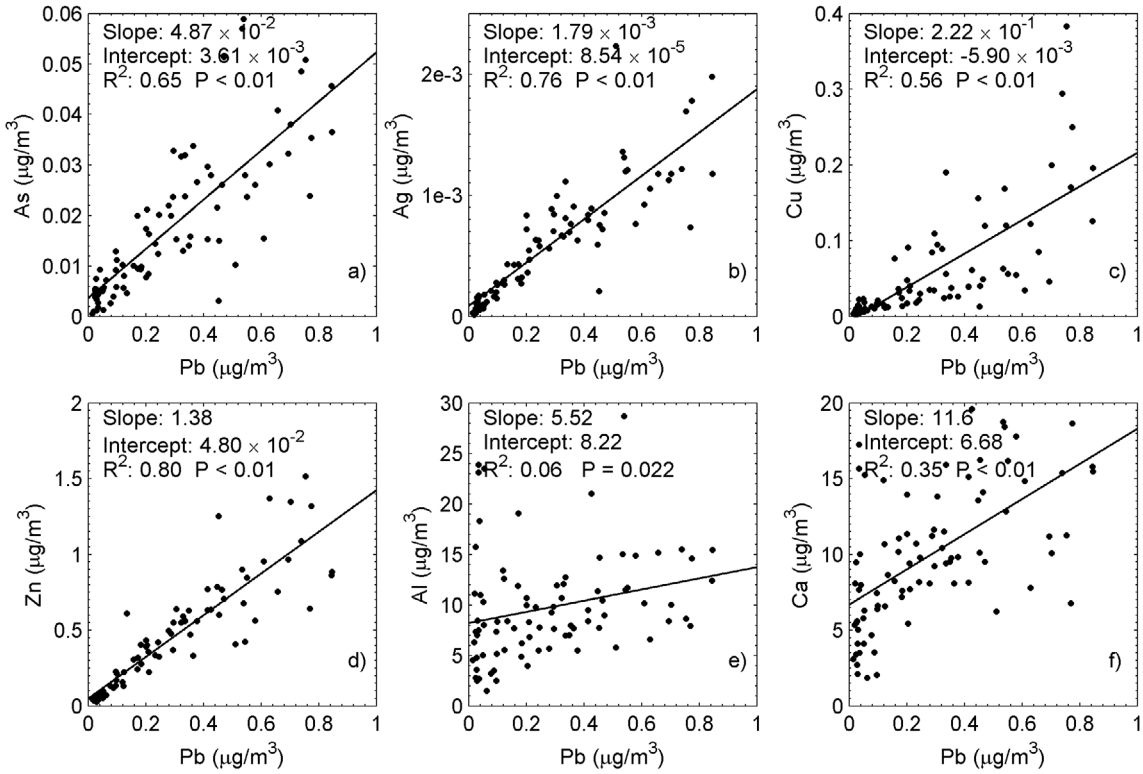

Figure 3. Scatterplots of (a) As and Pb, (b) Ag and Pb, (c) Cu and Pb, (d) Zn and Pb, (e) Al and Pb, and (f) Ca and Pb in aerosol samples collected in Xianghe during the experiment. Solid lines represent the least squares fits through the data. Correlation between Cu and Pb is derived after excluding two data points with abnormally high Cu.

used as tracers of anthropogenic aerosols [e.g., *Sun et al.*, 2005].

[17] Shown in Figure 1 are EFs of different elements in aerosol samples from Xianghe. Elements abundant in the Earth's crust like Ca, Fe, and Mg generally have EF below 5, and are mostly from soil sources, although human activities, for example, construction may also release aerosols containing Ca. Compared to Ca, Mg, and Fe, the EF of K is more variable, probably due to emissions from biomass burning, which will be discussed more in section 3.5. The EF of V is close to 1, showing little evidence of fuel oil combustion [*Rahn*, 1981]. Note that coal burning is by far the most important energy source in China [*China Bureau of Statistics*, 2008]. High EFs of As, Ag, Cd, and Pb indicate that they are largely derived from anthropogenic pollution sources. The element As may come from coal burning, incinerators, and smelters; Cd may be emitted from incinerators, smelters, and during manufacture of pigments [*Pacyna*, 1998]. The ambient levels of these pollution-related elements could be largely controlled by synoptic conditions, and their EFs are generally more variable than crustal elements.

3.3. Synoptic Change in Ambient Lead Levels

[18] Time series plots of Pb and its enrichment factor are given in Figures 2a and 2b, along with colocated measurements of CO and SO_2. The highly variable ambient abundance of Pb and its EF are well in phase with both gaseous pollutants (Figures 2a and 2b, Pb/CO R^2 = 0.50, Pb/SO_2 R^2 = 0.56), implying that they are generally from the same sources or source areas, and are largely controlled by the same regional-scale meteorological processes. While our time-resolved measurements such as trace gases reveal diurnal changes and local pollutant spikes controlled by the atmospheric boundary layer and small-scale meteorological processes [cf. *C. Li et al.*, 2007], the synoptic weather systems appear to be the far more important factor determining the pollutant levels during the experiment. The synoptic changes of trace gases observed in Xianghe have been discussed in detail elsewhere [*C. Li et al.*, 2007]. In short, cold fronts passing the area every 2–5 days during the experiment can be clearly identified from the meteorological records in Figures 2c and 2d, in particular from the strong northerly winds often accompanied by decreases in relative humidity. Pollutants (lead, CO, and SO_2) accumulate ahead of cold fronts, when low-speed winds blow from the populated and polluted area S/SW of Xianghe. After cold fronts sweep through the region, strong winds from less populated N/NW ventilate local emissions, bringing relatively clean air. The enrichment factor of Pb reaches as high as 400 during polluted episodes, and as low as 20 under postfrontal conditions, also suggesting that Pb measured in our aerosol samples is mainly from anthropogenic emission sources. Aerosols mainly consisting of soil/dust particles

Table 2. Compositions of Four Factors Resolved Using Unmix ($\mu g/m^3$)[a]

Species	Factor 1	Factor 2	Factor 3	Factor 4	Residue	R^2
Cl^-	0.62	**2.31**	0.57	−0.39	–	0.82
NO_3^-	0.13	2.57	**7.10**	−0.54	–	0.98
SO_4^{2-}	0.30	**2.15**	**4.02**	0.10	–	0.95
K^+	**1.06**	0.09	0.20	0.08	–	0.99
Mg	0.17	0.49	**0.71**	**1.71**	–	0.94
Al	−0.57	1.98	2.13	**6.03**	–	0.94
K	**1.15**	**0.97**	0.83	0.61	–	0.95
Ca	0.75	**2.35**	**2.77**	**3.92**	–	0.94
Zn	0.11	**0.36**	0.05	−0.10	–	0.92
Pb	0.03	**0.23**	0.07	−0.06	–	0.93
NH_4^+	0.22	1.98	2.74	0	0.16	0.91
$F^- \times 10^3$	34.8	63.0	53.2	0	0.00	0.90
$Mn \times 10^3$	13.5	68.0	34.5	42.9	8.73	0.90
$Ag \times 10^3$	0.06	0.36	0.16	0	0	0.89
$Th \times 10^3$	0	0.38	0.36	0.69	0	0.88
Fe	0.80	1.51	1.49	2.73	0	0.83
$Be \times 10^3$	0.02	0.15	0.05	0.10	0.07	0.83
$U \times 10^3$	0.03	0.20	0.06	0.07	0.08	0.81
$As \times 10^3$	0.18	13.6	3.27	0	0	0.76
$Ba \times 10^3$	1.04	42.0	21.2	24.7	1.70	0.75
Ca^{2+}	0.25	0.39	0.96	0.92	0.85	0.73
$Cd \times 10^3$	0.03	2.96	1.30	0	0	0.73
$Cu \times 10^3$	0.00	61.2	3.33	0	0	0.72
$Tl \times 10^3$	0.13	1.29	0.56	0	0	0.67
$Mg^{2+} \times 10^3$	1.83	56.0	82.7	87.4	70.8	0.58
Na	0.11	0.44	0.08	0.08	0.49	0.48
$V \times 10^3$	1.89	2.94	1.01	3.40	2.37	0.42
Na^+	0.07	0.18	0.04	0.07	0.25	0.33

[a]Values greater than 3 times the uncertainty estimated by Unmix are in boldface. Contributions of the four factors to species not included in the factor analysis (below Pb in the table) are estimated via multiple linear regression. The R^2 values indicate the correlation between predicated and measured concentrations.

behind cold fronts probably contain little lead and other anthropogenic pollutants.

3.4. Correlation Between Lead and Other Elements

[19] Results of correlation of Pb with a few selected elements are given in Figure 3. Good correlations are found between Pb and some trace elements including Zn (correlation coefficient, R^2 = 0.80), As (R^2 = 0.65), Ag (R^2 = 0.76), and Cu (R^2 = 0.56). These elements have some common sources with Pb, such as mining and processing of metals and waste incineration [e.g., *Nriagu and Pacyna*, 1988]. More importantly, these pollution-related trace elements may come from various sources and processes in the region that are all closely associated with anthropogenic activities. Pb is not correlated with Al, often used as a tracer of dust/soil particles [e.g., *Sun et al.*, 2005; *Wang et al.*, 2007]. Pb is moderately correlated with Ca (R^2 = 0.35); besides contributions from soil sources, Ca may also come from anthropogenic sources such as cement used in construction. Lime and limestone may be added during coal combustion to retain sulfur in coal. This may result in emissions of primary gypsum ($CaSO_4$) particles in the flue gas, as discussed in a companion paper employing electric microscope to study the same batch of aerosol samples [*Guo et al.*, 2010]. Combining limestone with coal has also been shown to enhance Pb emissions in some cases; limestone may contain lead and may also increase particle emissions [*Clarke*, 1993].

3.5. Unmix Resolved Sources

[20] Using concentrations of Cl^-, NO_3^-, SO_4^{2-}, K^+, Mg, Al, K, Ca, Zn, and Pb as input to the Unmix model, a unique four-factor solution is obtained (Table 2), which explains over 95% of the data variance. A few influential data points deemed to undermine the resolution of edges or source profiles by Unmix were automatically excluded from the model calculation [*U.S. EPA*, 2007b], including Cl^- in the nighttime sample on DOY 79, SO_4^{2-} in the daytime samples on DOY 95 and 96, and Zn in the nighttime sample on DOY 88. Adding one or more species such as Cu, As, Ag, F^-, Fe, Na, and Ca^{2+} to the model input generates very similar results with four factors. Unmix evaluates the uncertainties in the resolved source profiles using boot-strapping methods [*U.S. EPA*, 2007b]. Species with model-estimated contribution greater than three times the model-calculated uncertainty are marked in bold in Table 2. Source contributions to species not included in the model input are determined with multiple linear regression. The results are also given in Table 2.

[21] The most important tracer species in Factor 1, K^+ and K, have similar concentrations, implying the noncrustal origin of K in this factor. Water-soluble K^+ is a tracer of biomass burning emissions [e.g., *Duan et al.*, 2004], and agricultural fires near the sampling site were often spotted during the field experiment [*C. Li et al.*, 2007], particularly around early and middle March, before the local agricultural activities pick up. In addition, biofuels are common in the area for domestic use. Another important species in Factor 1 is Zn, with concentration greater than twice the model uncertainty. *Gaudichet et al.* [1995] observed substantial emissions of Zn from tropical African savanna fires. The contribution to aerosols by Factor 1, estimated by Unmix and shown as solid red squares in Figure 4a, demonstrates synoptic change generally similar to that of lead and trace gases (Figure 2), as stagnant conditions favor buildup of fire-related pollutants. Also agricultural fires may be less intense under windy conditions for safety reasons.

[22] Factor 2 is the largest source of Pb, Zn, and Cl^-, and a significant source of SO_4^{2-}, K, and Ca. Several elements not included as Unmix input but can be used as tracers of industrial processes and coal combustion, such as Ag, As, Cd, Cu, and Tl, also find Factor 2 as their major contributor (Table 2). This factor probably mainly reflects primary emissions from industrial activities and (relatively small-scale low-temperature) coal combustion such as home heating and institutional boilers. Cl^- is enriched in reference to Na^+, and more so when the concentration of SO_2, mostly from coal burning, is higher (Figure 5). Previous studies in Beijing [e.g., *Wang et al.*, 2005] recognize coal burning in this area as a main source of airborne Cl^-. Over polluted continental areas, anthropogenic emissions may lead to generation of highly reactive atomic chlorine [*Thornton et al.*, 2010]. Pb may also enter the atmosphere as $PbCl_2$, a product of burning low-class coal [*U.S. EPA*, 2007a]. The existence of Ca and SO_4^{2-} in this factor is interesting: as already discussed, Ca-containing materials (e.g., lime and lime stone) are probably introduced during coal combustion to control SO_2 emissions. Gypsum, among other primary sulfate aerosols, may make up a good fraction of the total sulfate observed in this region [*Guo et al.*, 2010].

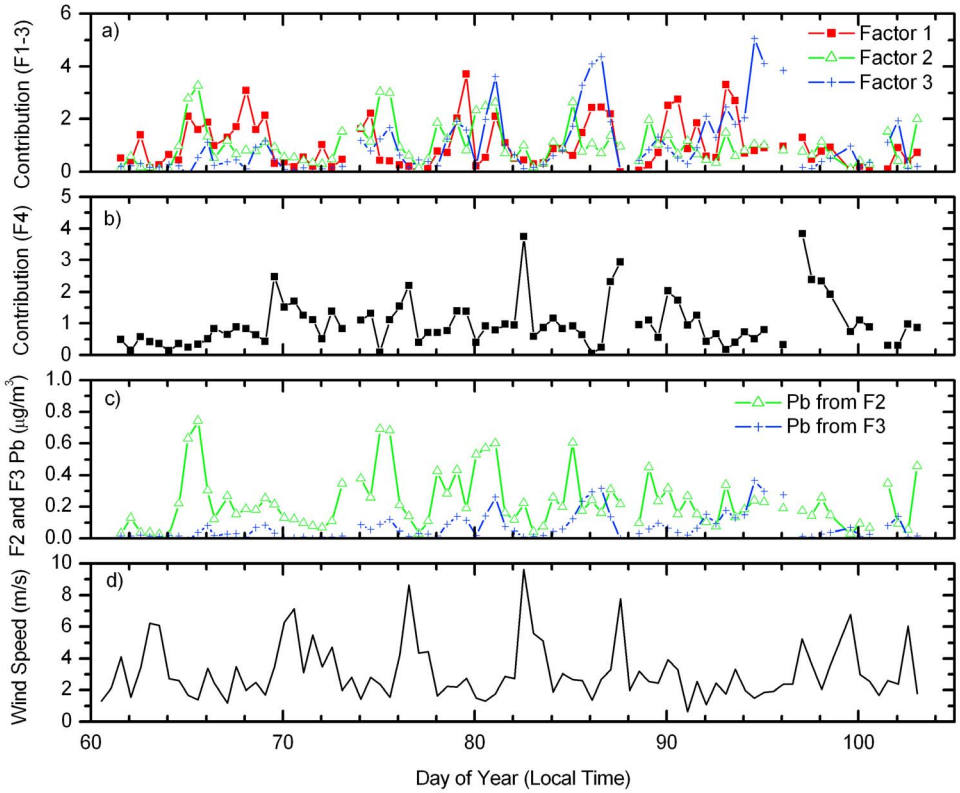

Figure 4. (a) Contributions of Factors 1–3 to Xianghe bulk aerosol samples as resolved by Unmix. Gaps in the time series are due to outliers removed by the Unmix receptor model (see section 3.5). One unit in source contribution from Factor 1, as an example, indicates that 1.06 $\mu g/m^3$ K^+, and 0.62 $\mu g/m^3$ Cl^-, among other species, are from Factor 1 type of sources. (b) Source contribution of Factor 4. (c) Lead contributed by Factor 2 and Factor 3 resolved by Unmix. (d) Wind speed at the Xianghe site during the experiment.

Like Factor 1, Factor 2 also demonstrates synoptic variation (green triangles, Figure 4a) similar to that of SO_2 and CO. Over the whole experiment, the strength of Factor 2 appears to decrease with time. The reasons may be twofold: as temperature goes up heading from late winter into spring (Figure 2), the less stable atmosphere assists faster removal of primary pollutants from their sources, meanwhile demand for space heating weakens, as does small-scale coal burning. Note that we cannot completely rule out the contribution from resuspended soil particles with heavy metal contamination (e.g., previously emitted Pb deposited to soil) in this factor, although it is likely minor as our site is at least 500 m away from any major roads, and weak winds would mobilize few soil particles. Mobile source emissions in this region may also contribute to this factor: Zn has been proposed as a tracer for mobile sources after the phase out of leaded gasoline [*Huang et al.*, 1994], and older vehicles can still emit lead. But our site is expected to be much less influenced by mobile emissions owing to its nonurban location. Zn may come from industrial sources; the existence of other species also suggests that automobiles are not likely the dominant source for this factor. To resolve a distinct mobile factor, more time-resolved samples and analysis of tracers predominantly emitted by mobile sources may be necessary.

[23] With NO_3^- and SO_4^{2-} as the major tracer species, Factor 3 mainly represents secondary aerosols, which also contribute most of the NH_4^+ and a considerable fraction of Ca, Ca^{2+} and Mg (Table 2). While NH_4^+ (Table 1) is the major species neutralizing the anions in our aerosol samples, HNO_3 gas generated via photochemical processes may also combine with the abundant soil particles (e.g., calcium carbonate) in the air to form nitrate aerosols. The relatively high $[NO_3^-]/[SO_4^{2-}]$ ratio also suggests high-temperature coal combustion sources such as electricity generation. As with Factors 1 and 2, Factor 3 (blue plus, Figure 4a) is greater ahead of cold fronts and smaller behind them. Unlike Factors 1 and 2, Factor 3 demonstrates an upward seasonal trend over time during the sampling period. This probably reflects more active photochemical activities as warmer temperature (Figure 1) and stronger sunlight facilitate generation of secondary pollutants. The high-temperature coal combustion in Factor 3 also contributes to a small fraction of Pb and Zn, especially in early April when Factor 2 becomes relatively small while Factor 3 is at its peak (Figure 4c). But the results need to be interpreted with caution due to uncertainties in Unmix. Combined, Factors 2 and 3 comprise over 90% of the Pb observed in this study.

[24] Factor 4 features high levels of Mg, Al, and Ca, all typical crustal elements associated with dust and soil parti-

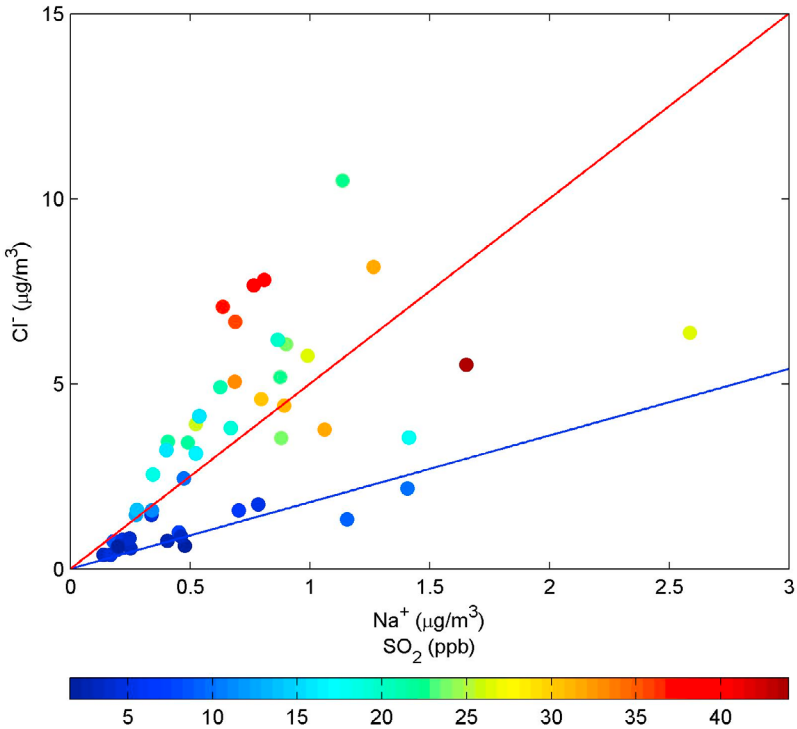

Figure 5. Scatterplot of Cl^- and Na^+ concentrations. Color of the dots represents the average SO_2 concentration for the corresponding samples. Blue (slope = 1.8) and red (slope = 5) solid lines are for reference only. Cl^- is likely mainly from small-scale relatively low technology coal burning.

cles. Fe, not included in model calculation, also predominantly comes from Factor 4. Different from Factors 1–3, Factor 4 is strongest under windy postfrontal conditions (correlation with wind speed: $R > 0.5$, $P < 0.01$), and weakest in the stagnant prefrontal environment. In spring, intense NW winds may bring to this area very lightly polluted dust from the Gobi deserts and other dust source regions. Local dust emissions from bare agricultural land in early spring may also pick up as cold fronts sweep through the area with strong winds. Compared to Factors 2 and 3, which have Al/Ca mass ratios of ~0.9, Factor 4 has a much higher Al/Ca ratio of ~1.5, similar to the aerosol samples collected near the Gobi desert [e.g., *Zhang et al.*, 2003a] and eastern Inner Mongolia [e.g., *Huang et al.*, 2010; *Sun et al.*, 2010]. Small negative values for Zn and Pb, allowed by Unmix as discussed in section 2, imply from none to little contribution by dust aerosols to the pollution-derived trace elements. Based on the results of the Unmix model, we conclude that Pb in aerosols in this study is mainly emitted from industrial processes and coal burning.

3.6. Potential Source Contribution Function

[25] The potential source contribution function, PSCF, calculated using equation (1) based on HYSPLIT-generated backward trajectories and the criterion for Pb concentration (Pb ≥ 0.4 $\mu g/m^3$) in aerosol samples, is shown in Figure 6a. Figures 6b and 6c present the PSCFs calculated with the criteria for enrichment factor of Pb (EF of Pb ≥ 125) and for the source strength of Factor 2 from Unmix results (Factor 2 contribution ≥ 1, i.e., Pb from Factor 2 ≥ 0.23 $\mu g/m^3$), respectively. As can be seen from Figure 6, PSCFs using three different criteria show similar spatial patterns, with hot spots distributed to the south and SW and lower values to the north and NW of Xianghe. To the S/SW of our measurement site is one of the most populated and industrialized regions in China, having been identified as major source regions of air pollutants in satellite observations [e.g., *Krotkov et al.*, 2008], and bottom-up emission inventories [e.g., *Streets et al.*, 2003; *Q. Zhang et al.*, 2009]. For comparison, Figure 7d depicts the industrial SO_2 source estimated for 2006 [*Q. Zhang et al.*, 2009]. The high PSCFs and strong industrial emissions to the S/SW of Xianghe indicate that the manufacturing industries and coal combustion in this region are among the most important sources of Pb in this study.

[26] PSCF as defined in equation (1) does not take into account the height of the trajectories along the transport pathway. On the other hand, air parcels traveling at lower altitudes, in the boundary layer have more chances to contact and carry pollutants, which are mostly emitted near ground. We define a modified potential source contribution function as follows:

$$PSCF'_{ij} = {m'_{ij}} \Big/ {n'_{ij}}, \tag{3}$$

where $PSCF'_{ij}$ is the modified $PSCF$, m'_{ij} and n'_{ij} are similar to their counterparts in equation 1, but only account for trajectory endpoints within 1000 m above the surface.

[27] Figure 7 shows the modified PSCFs. Trajectories from the north and northwest are normally associated with

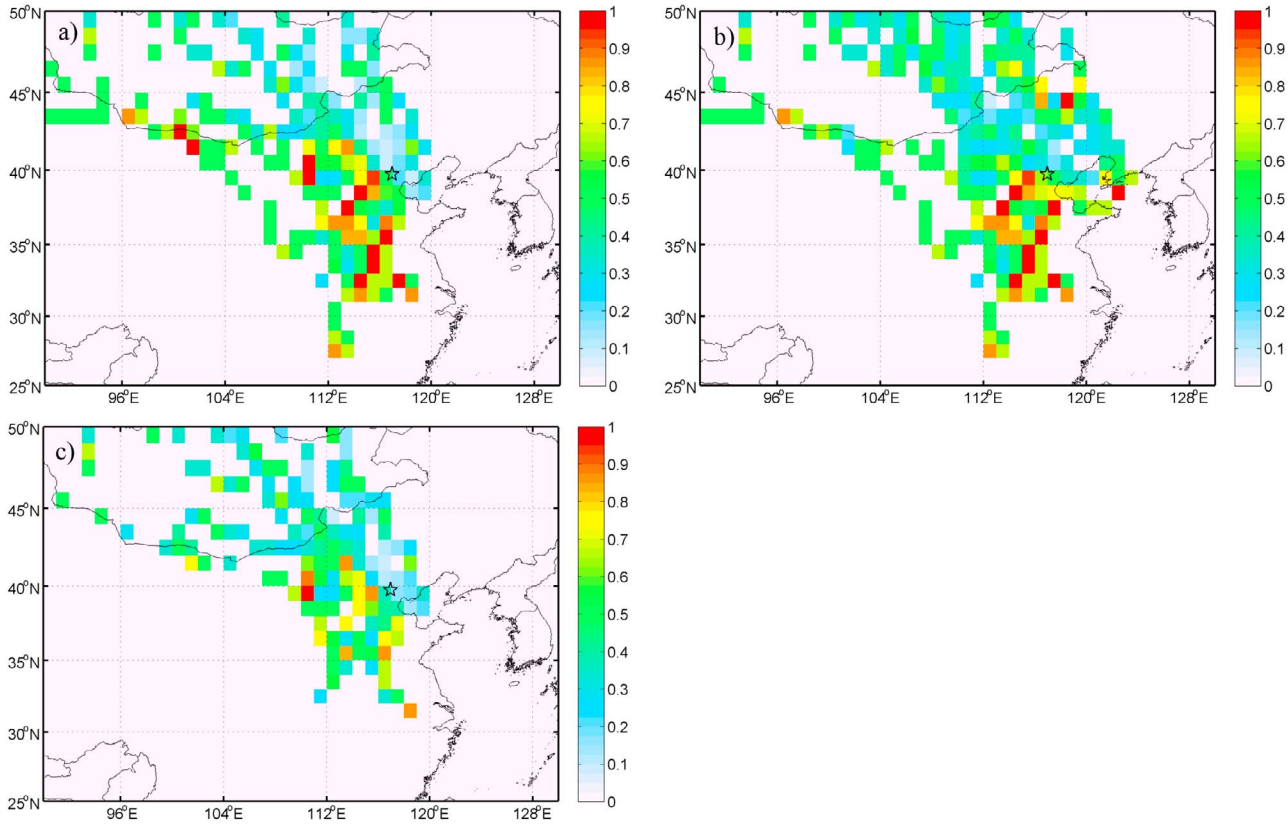

Figure 6. Potential source contribution function (PSCF) calculated based on equation (1), using 72 h backward trajectories, and criteria for (a) Pb concentration, (b) enrichment factor of Pb, and (c) strength of Factor 2 resolved with the Unmix model. High PSCF values to the south and SW of Xianghe (star) suggest that ambient Pb observed in this study is mainly from this populated and industrialized region of China.

high-pressure systems and descending motion; and the modified PSCFs exclude a number of trajectory endpoints from that direction. The modified PSCFs for the sector to the south and SW of Xianghe are quite similar to the PSCFs in Figure 6, confirming that the industrial emissions (Figure 7d) and coal combustion from that region could be the main source of our observed ambient Pb.

4. Discussion: Atmospheric Particulate Lead in China

[28] It is enlightening to compare the lead levels in Xianghe to other areas in China, although direct comparison is complicated by differences in analytical methods, sampling time, strategy, and size. Table 3 gives the Pb concentrations and enrichment factors at different locations in China, summarized from studies mostly conducted in the eastern part of China after the phase out of leaded gasoline. Among the measurement sites listed in the table, Tongliao, Duolun, Zhenbeitai, Daihai, and Yulin are sites located in less populated arid and semiarid areas close to deserts. The Pb concentrations at these sites are generally below 0.1 μg/m^3. The EF of Pb in springtime bulk aerosol samples from Zhenbeitai is ~20, close to our observed EF behind cold fronts, when dust particles carried by NW winds prevail. Such low Pb concentrations and enrichment factors may probably represent the background Pb levels in northern China. Beijing, Shanghai, and Guangzhou, on the contrary, are the largest and most developed cities in China, featuring generally PM_{10} or bulk Pb concentrations of 0.15 μg/m^3 or higher in cold seasons (spring and winter). Enrichment factors of Pb for these cities are mostly over 100 in bulk and PM_{10} aerosol samples and even higher in fine particles ($PM_{2.5}$). Lianyungang and Qingdao are both coastal cities with some heavy industry; bulk aerosol Pb levels measured in the two cities are mostly > 0.1 μg/m^3 and higher in winter. Wuhan and Urumuqi, two industrialized big cities in central and northwestern China, record Pb levels around 0.5 μg/m^3 in PM_{10} and bulk aerosol samples, respectively. The sites in industrial districts of big cities generally have the greatest Pb concentrations, indicative of the industrial origins of ambient Pb. Pb levels at suburban locations tend to be lower than at urban/industrial sites, but can still be substantial. For example, at the suburban site ~100 km north of Beijing, *Sun et al.* [2006] found the springtime bulk aerosol Pb level at ~0.15 μg/m^3, smaller than but comparable to 0.28 μg/m^3 observed in this study. Much of Pb resides in fine particles, implying that emissions from combustion and other industrial processes are probably the most important sources of ambient Pb, although coarse-mode Pb increases

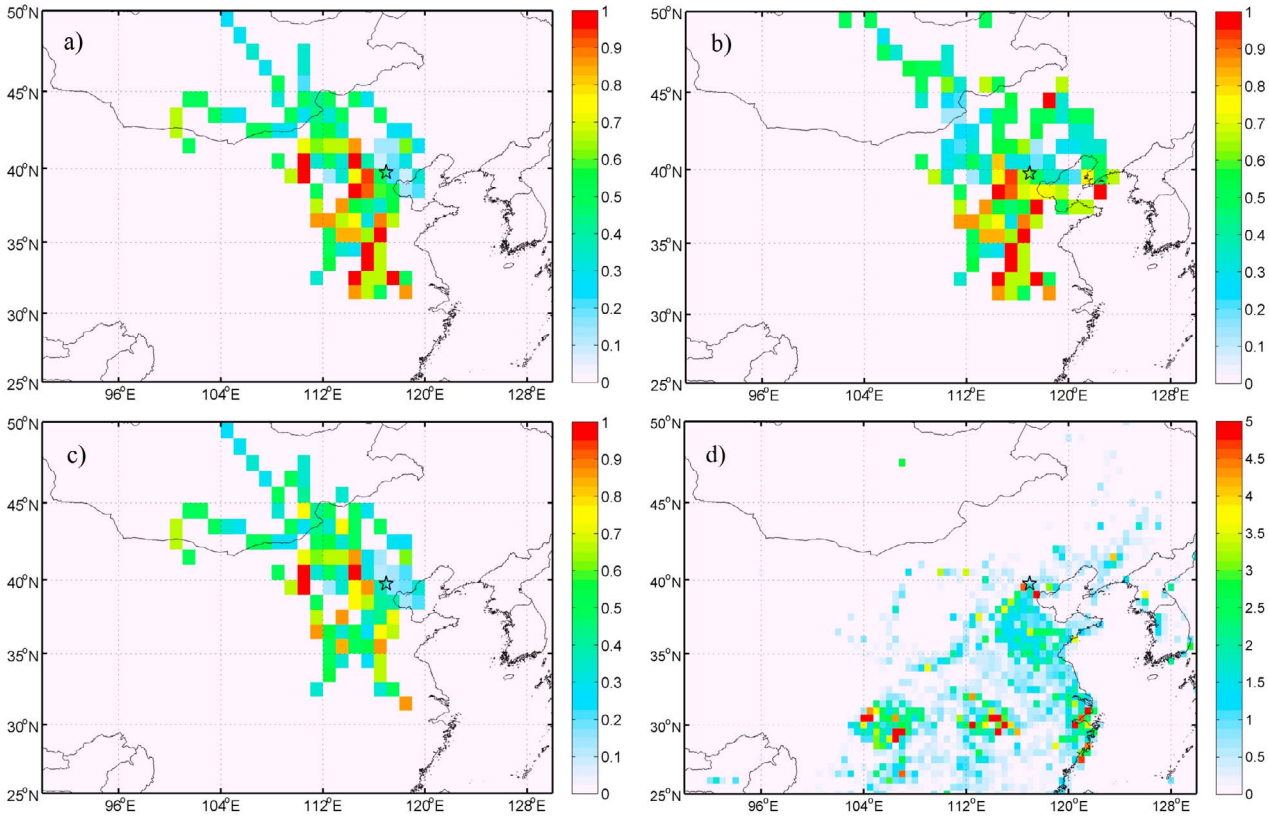

Figure 7. (a, b, and c) Same as Figure 6 but for modified PSCF defined in equation (3), in which only trajectory endpoints below 1000 m above ground are taken into consideration. (d) Industrial SO_2 emissions (10^4 tonne/y per 0.5° × 0.5° grid cell) estimated for 2006 [*Q. Zhang et al.*, 2009].

in spring, as generally stronger winds mobilize Pb-containing soil particles. Overall, recently reported ambient Pb levels in east China are in accordance with the air quality standard of China, but sizable in both urban and suburban areas.

5. Conclusions

[29] In this study bulk aerosol samples collected in Xianghe, a rural site ~70 km ESE of Beijing, in spring 2005 were analyzed for major elements and water-soluble inorganic ions. Substantial amounts of crustal elements (e.g., Al) were observed, along with considerable loadings of secondary aerosol species (e.g., nitrate). Both soil particles and anthropogenic sources contributed to aerosol loadings in this area in spring. The average concentration of lead during the experiment was 0.28 $\mu g/m^3$, and highly enriched (average EF > 100) relative to the Earth's crust. This concentration is above the current U.S. ambient standard but below the average value seen in the U.S. when leaded gasoline was in common use. Lead levels were well-correlated with CO and SO_2, demonstrating large variation with weather conditions. The good correlation between Pb and pollution-related elements suggests that the ambient lead observed in this study was mainly released from human activities.

[30] Four factors were resolved through a factor analysis of the aerosol composition data utilizing the EPA Unmix receptor model. Three factors contribute a large fraction of the aerosol loadings under prefrontal conditions: a biomass burning source (Factor 1) likely associated with agricultural fires and biofuel burning around the site; a source (Factor 2) which contributes the majority of Pb and several other pollutant trace elements as well as Cl^-, mainly representing emissions of industrial processes and small-scale relatively low technology coal combustion such as in home and institutional heating; and a source (Factor 3) reflecting the secondary species (sulfate and nitrate) possibly related to high-temperature coal burning (e.g., electricity generation). Vehicle emissions may also contribute to Factor 2, but are not likely the dominant source. Factors 2 and 3 make up over 90% of the lead observed during the experiment. The final source (Factor 4) represents dust particles carried by strong northerly winds into the area, and has little influence on lead concentration. Our results that lead mainly comes from industrial processes and coal combustion instead of vehicular emissions agree with several previous studies in China involving measurements of lead isotopes [e.g., *Chen et al.*, 2008], and aerosol source apportionment [e.g., *Bi et al.*, 2007; *Lv et al.*, 2006; *Sun et al.*, 2006].

[31] The potential source contribution function (PSCF) was calculated using Pb concentration, enrichment factor, and the strength of Factor 2 resolved by Unmix as criteria. High values of PSCFs were generally found in the areas to

Table 3. Concentration and Enrichment Factor of Lead in Aerosol Samples From Various Sites in China in Recent Years[a]

Location	Sampling Period	Site Type	Sample Size	Season/ Month	Pb ($\mu g/m^3$)	Enrichment Factor	Reference
Xianghe, north China	Mar–Apr 2005	Rural/Suburban	Bulk		0.280	115	This study
Lianyungang, east China	Jun–Dec 2003	Urban/Coastal	Bulk	summer	0.120	167[b]	*Zhang et al.* [2005]
	Jun–Dec 2003	Urban/Coastal	Bulk	fall	0.190	189[b]	*Zhang et al.* [2005]
	Jun–Dec 2003	Urban/Coastal	Bulk	Dec	0.570	265[b]	*Zhang et al.* [2005]
Tongliao, NE China	Jun–Sep 2003	Near desert	Bulk	summer	0.080	173[b]	*Zhang et al.* [2005]
	Mar–May 2005	Near desert	$PM_{2.5}$	spring	0.125	132	*Shen et al.* [2007]
Duolun, north China	2003–2004	Urban/Small town	$PM_{2.5}$	spring	0.029	N/A	*Sun et al.* [2006]
	2003–2004	Urban/Small town	$PM_{2.5}$	fall	0.034	N/A	*Sun et al.* [2006]
	2003–2004	Urban/Small town	Bulk	spring	0.030	N/A	*Sun et al.* [2006]
	2003–2004	Urban/Small town	Bulk	fall	0.028	N/A	*Sun et al.* [2006]
Urumqi, NW China	2004–2008	Urban	$PM_{2.5}$		0.360	1055	*Li et al.* [2008]
	2004–2008	Urban	Bulk		0.450	225	*Li et al.* [2008]
Zhenbeitai, north China	Apr 2001	Near desert	$PM_{2.5}$	spring	0.023	60	*Arimoto et al.* [2004]
	Feb–May 2001	Near desert	Bulk	spring	0.064	18	*Zhang et al.* [2003b]
Yulin, north China	Spring 2004	Near desert	$PM_{2.5}$	spring	0.043	N/A	*Sun et al.* [2006]
	Spring 2004	Near desert	Bulk	spring	0.070	N/A	*Sun et al.* [2006]
Daihai, north China	June–July 2006	Rural	Bulk	summer	0.044	70[b]	*Han et al.* [2009]
	June–July 2006	Rural	$PM_{2.5}$	summer	0.020	270[b]	*Han et al.* [2009]
Beijing, north China	2002–2003	Urban	PM_{10}	winter	0.370	367	*Sun et al.* [2004]
	2002–2003	Urban	PM_{10}	summer	0.110	83	*Sun et al.* [2004]
	2002–2003	Industrial	PM_{10}	winter	0.460	304	*Sun et al.* [2004]
	2002–2003	Industrial	PM_{10}	summer	0.220	185	*Sun et al.* [2004]
	2002–2003	Residential	PM_{10}	winter	0.490	355	*Sun et al.* [2004]
	2002–2003	Residential	PM_{10}	summer	0.110	131	*Sun et al.* [2004]
	Spring 2004	Urban	$PM_{2.5}$	spring	0.176	N/A	*Sun et al.* [2006]
	Spring 2004	Urban	Bulk	spring	0.307	N/A	*Sun et al.* [2006]
	Spring 2004	Suburban	$PM_{2.5}$	spring	0.195	N/A	*Sun et al.* [2006]
	Spring 2004	Suburban	Bulk	spring	0.147	N/A	*Sun et al.* [2006]
Qingdao, north China	Jun 2001 to May 2002	Urban/coastal	Bulk	winter	0.315	391[b]	*Hao et al.* [2007]
	Jun 2001 to May 2002	Urban/coastal	Bulk	dust	0.185	26[b]	*Hao et al.* [2007]
	Jun 2001 to May 2002	Urban/coastal	Bulk	summer	0.064	231[b]	*Hao et al.* [2007]
	Jun 2001 to May 2002	Urban/coastal	Bulk	spring	0.101	160[b]	*Hao et al.* [2007]
	Jun 2001 to May 2002	Urban/coastal	Bulk	fall	0.166	209[b]	*Hao et al.* [2007]
	Jun 2003	Urban/coastal	Bulk	summer	0.110	248	*Lammel et al.* [2006]
	Spring 2004	Urban/coastal	Bulk	spring	0.156	N/A	*Sun et al.* [2004]
Wuhan, central China	2003–2004	Urban	PM_{10}		0.409	443	*Lv et al.* [2006]; *Querol et al.* [2006]
	2003–2004	Industrial	PM_{10}		0.615	424	*Lv et al.* [2006]; *Querol et al.* [2006]
	2003–2004	Rural/Suburban	PM_{10}		0.151	286	*Lv et al.* [2006]; *Querol et al.* [2006]
Shanghai, east China	Mar 1999 to Mar 2000	Urban/downtown	$PM_{2.5}$	summer	0.160	2008	*Ye et al.* [2003]
	Mar 1999 to Mar 2000	Urban/downtown	$PM_{2.5}$	fall	0.320	2989	*Ye et al.* [2003]
	Mar 1999 to Mar 2000	Urban/downtown	$PM_{2.5}$	winter	0.400	2362	*Ye et al.* [2003]
	Mar 1999 to Mar 2000	Urban	$PM_{2.5}$	spring	0.230	1679	*Ye et al.* [2003]
	Mar 1999 to Mar 2000	Urban	$PM_{2.5}$	summer	0.160	2471	*Ye et al.* [2003]
	Mar 1999 to Mar 2000	Urban	$PM_{2.5}$	fall	0.320	2921	*Ye et al.* [2003]
	Mar 1999 to Mar 2000	Urban	$PM_{2.5}$	winter	0.370	2519	*Ye et al.* [2003]
	2003–2004	Urban	$PM_{2.5}$	spring	0.086	N/A	*Sun et al.* [2006]
	2003–2004	Urban	$PM_{2.5}$	fall	0.039	N/A	*Sun et al.* [2006]
	2003–2004	Urban	Bulk	spring	0.176	N/A	*Sun et al.* [2006]
	2003–2004	Urban	Bulk	fall	0.046	N/A	*Sun et al.* [2006]
	April 2004 to April 2005	Suburban	$PM_{2.5}$		0.067	167[c]	*Chen et al.* [2008]
	April 2004 to April 2005	Industrial	$PM_{2.5}$		0.149	198[c]	*Chen et al.* [2008]
	April 2004 to April 2005	Urban	$PM_{2.5}$		0.143	220[c]	*Chen et al.* [2008]
	April 2004 to April 2005	Urban	$PM_{2.5}$		0.075	136[c]	*Chen et al.* [2008]
Guangzhou, south China	Aug–Sep 2004	Urban	PM_{10}	summer	0.466	280	*X. Wang et al.* [2006]
	Aug–Sep 2004	Urban	PM_{10}	summer	0.342	170	*X. Wang et al.* [2006]
	Aug–Sep 2004	Urban	PM_{10}	summer	0.425	341	*X. Wang et al.* [2006]
	Aug–Sep 2004	Suburban	PM_{10}	summer	0.324	303	*X. Wang et al.* [2006]
	Dec 2003 to Jan 2005	Urban	Bulk	winter	0.269	319	*Lee et al.* [2007]
	Dec 2003 to Jan 2005	Suburban	Bulk	winter	0.219	313	*Lee et al.* [2007]
Shenzhen, south China	Oct 2002 to Jun 2003	Urban	$PM_{2.5}$		0.016	643	*Hagler et al.* [2007]
Zhongshan, south China	Oct 2002 to Jun 2003	Suburban	$PM_{2.5}$		0.020	574	*Hagler et al.* [2007]
Conghua, south China	Oct 2002 to Jun 2003	Rural	$PM_{2.5}$		0.023	577	*Hagler et al.* [2007]
Guangzhou, south China	Oct 2002 to Jun 2003	Urban	$PM_{2.5}$		0.030	446	*Hagler et al.* [2007]
Pearl River estuary, south China	Jan and Apr 2003	Cruise	$PM_{2.5}$	winter	0.189	3041	*Zhang et al.* [2007]
	Jan and Apr 2003	Cruise	$PM_{2.5}$	spring	0.020	419	*Zhang et al.* [2007]

[a]Enrichment factors are calculated using Al as the reference element unless otherwise noted.
[b]Reference element: Fe.
[c]Reference element: Ti.

the south and SW of Xianghe, a populated and industrialized region with strong pollutant emissions [e.g., *Krotkov et al.*, 2008; *Q. Zhang et al.*, 2009]. Vehicular emissions from Beijing to the west are not likely an important source of Pb in Xianghe.

[32] Similar to Xianghe, Pb levels at other suburban sites near big cities in China are generally lower than those observed in industrial districts and downtown areas, but are near or above the new U.S. standard. Ambient lead concentrations at sites near the dust source areas in western China are much lower. Pb in the eastern part of China is likely mainly derived from local and regional anthropogenic sources. Limited analyses indicate moderate Pb content in coal samples from China [*Díaz-Somoano et al.*, 2009], but the coal consumption in China reached almost three billion tonne/yr [*China Bureau of Statistics*, 2008], and likely will further increase in the future. More extensive studies of airborne lead and measurements of lead emission rates from various types of sources will be essential for better understanding and controlling lead in China.

[33] **Acknowledgments.** We thank Dennis Savoie and Joseph Prospero of the University of Miami for helping design the aerosol sampler. This study was supported by MOST (2006CB403706), NASA (NNG04GE79G), DOE (DEFG0208ER64571), and NSF (ATM0412040).

References

Arimoto, R., X. Y. Zhang, B. J. Huebert, C. H. Kang, D. L. Savoie, J. M. Prospero, S. K. Sage, C. A. Schloesslin, H. M. Khaing, and S. N. Oh (2004), Chemical composition of atmospheric aerosols from Zhenbeitai, China, and Gosan, South Korea, during ACE-Asia, *J. Geophys. Res.*, *109*, D19S04, doi:10.1029/2003JD004323.

Begum, B. A., E. Kim, C.-H. Jeong, D.-W. Lee, and P. K. Hopke (2005), Evaluation of the potential source contribution function using the 2002 Quebec forest fire episode, *Atmos. Environ.*, *39*, 3719–3724, doi:10.1016/j.atmosenv.2005.03.008.

Bi, X., Y. Feng, J. Wu, Y. Wang, and T. Zhu (2007), Source apportionment of PM_{10} in six cities of northern China, *Atmos. Environ.*, *41*, 903–912, doi:10.1016/j.atmosenv.2006.09.033.

Chen, J., F. Wei, C. Zheng, Y. Wu, and D. C. Adriano (1991), Background concentrations of elements in soils of China, *Water Air Soil Pollut.57–58*, 699–712, doi:10.1007/BF00282934.

Chen, J., M. Tan, Y. Li, Y. Zhang, W. Lu, Y. Tong, G. Zhang, and Y. Li (2005), A lead isotope record of Shanghai atmospheric lead emissions in total suspended particles during the period of phasing out of leaded gasoline, *Atmos. Environ.*, *39*, 1245–1253, doi:10.1016/j.atmosenv.2004.10.041.

Chen, J., M. Tan, Y. Li, J. Zheng, Y. Zhang, Z. Shan, G. Zhang, and Y. Li (2008), Characteristics of trace elements and lead isotope ratios in PM2.5 from four sites in Shanghai, *J. Hazard. Mater.*, *156*, 36–43, doi:10.1016/j.jhazmat.2007.11.122.

Chen, L.-W. A., B. G. Doddridge, R. R. Dickerson, J. C. Chow, and R. C. Henry (2002), Origins of fine aerosol mass in the Baltimore-Washington corridor: Implications from observation, factor analysis, and ensemble air parcel back trajectories, *Atmos. Environ.*, *36*, 4541–4554, doi:10.1016/S1352-2310(02)00399-0.

China Bureau of Statistics (2008), *China Statistical Yearbook 2008*, China Stat., Beijing, China.

China Ministry of Environmental Protection (1996), *National Ambient Air Quality Standards of China*, Beijing, China.

Clarke, L. B. (1993), The fate of trace elements during coal combustion and gasification: An overview, *Fuel*, *72*, 731–736, doi:10.1016/0016-2361(93)90072-A.

Díaz-Somoano, M., M. E. Kylander, M. A. López-Antón, I. Suárez-Ruiz, M. R. Martínez-Tarazona, M. Ferrat, B. Kober, and D. J. Weiss (2009), Stable lead isotope compositions in selected coals from around the world and implications for present day aerosol source tracing, *Environ. Sci. Technol.*, *43*, 1078–1085, doi:10.1021/es801818r.

Dickerson, R. R., and A. C. Delany (1988), Modification of a commercial gas filter correlation CO detector for enhanced sensitivity, *J. Atmos. Oceanic Technol.*, *5*, 424–431, doi:10.1175/1520-0426(1988)005<0424:MOACGF>2.0.CO;2.

Duan, F., X. Liu, T. Yu, and H. Cachie (2004), Identification and estimate of biomass burning contribution to the urban aerosol organic carbon concentrations in Beijing, *Atmos. Environ.*, *38*, 1275–1282, doi:10.1016/j.atmosenv.2003.11.037.

Ehrman, S. H., S. E. Pratsinis, and J. R. Young (1992), Receptor modeling of the fine aerosol at a residential Los Angeles site, *Atmos. Environ. Part B*, *26*, 473–481.

Fang, G.-C., Y.-S. Wu, S.-H. Huang, and J.-Y. Rau (2005), Review of atmospheric metallic elements in Asia during 2000–2004, *Atmos. Environ.*, *39*, 3003–3013, doi:10.1016/j.atmosenv.2005.01.042.

Gaudichet, A., F. Echalar, B. Chatenet, J. P. Quisefit, and G. Malingre (1995), Trace elements in tropical African savanna biomass burning aerosols, *J. Atmos. Chem.*, *22*, 19–39, doi:10.1007/BF00708179.

Guo, Z., Z. Li, J. Farquhar, A. J. Kaufman, N. Wu, C. Li, R. R. Dickerson, and Wang Pl (2010), Identification of sources and formation processes of atmospheric sulfate by sulfur isotope and scanning electron microscope measurements, *J. Geophys. Res.*, *115*, D00K07, doi:10.1029/2009JD012893.

Hagler, G. S. W., M. H. Bergin, L. G. Salmon, J. Z. Yu, E. C. H. Wan, M. Zheng, L. M. Zeng, C. S. Kiang, Y. H. Zhang, and J. J. Schauer (2007), Local and regional anthropogenic influence on PM2.5 elements in Hong Kong, *Atmos. Environ.*, *41*, 5994–6004, doi:10.1016/j.atmosenv.2007.03.012.

Han, Y. M., J. J. Cao, Z. D. Jin, and Z. S. An (2009), Elemental composition of aerosols in Daihai, a rural area in the front boundary of the summer Asian Monsoon, *Atmos. Res.*, *92*, 229–235, doi:10.1016/j.atmosres.2008.10.031.

Hao, Y., Z. Guo, Z. Yang, M. Fang, and J. Feng (2007), Seasonal variations and sources of various elements in the atmospheric aerosols in Qingdao, China, *Atmos. Environ.*, *85*, 27–37.

Harris, A. R., and C. I. Davidson (2005), The role of resuspended soil in lead flows in the California South Coast Air Basin, *Environ. Sci. Technol.*, *39*, 7410–7415, doi:10.1021/es050642s.

Henry, R. C. (1997), History and fundamentals of multivariate air quality receptor models, *Chemom. Intell. Lab. Syst.*, *37*, 37–42, doi:10.1016/S0169-7439(96)00048-2.

Henry, R. C., E. S. Park, and C. H. Spiegelman (1999), Comparing a new algorithm with the classic methods for estimating the number of factors, *Chemom. Intell. Lab. Syst.*, *48*, 91–97, doi:10.1016/S0169-7439(99)00015-5.

Hu, S., R. McDonald, D. Martuzevicius, P. Biswas, S. A. Grinshpun, A. Kelley, T. Reponen, J. Lockey, and C. LeMasters (2006), Unmix modeling of ambient $PM_{2.5}$ near an interstate highway in Cincinnati, OH, USA, *Atmos. Environ.*, *40*, Suppl. 2, 378–395, doi:10.1016/j.atmosenv.2006.02.038.

Huang, K., G. Zhuang, J. Li, Q. Wang, Y. Sun, Y. Lin, and J. S. Fu (2010), Mixing of Asian dust with pollution aerosol and the transformation of aerosol components during the dust storm over China in spring 2007, *J. Geophys. Res.*, *115*, D00K13, doi:10.1029/2009JD013145.

Huang, X., I. Olmez, N. K. Aras, and G. E. Gordon (1994), Emissions of trace elements from motor vehicles: Potential marker elements and source composition profile, *Atmos. Environ.*, *28*, 1385–1391, doi:10.1016/1352-2310(94)90201-1.

Huo, X., L. Peng, X. Xu, L. Zheng, B. Qiu, Z. Qi, B. Zhang, D. Han, and Z. Piao (2007), Elevated blood lead levels of children in Guiyu, an electronic waste recycling town in China, *Environ. Health Perspect.*, *115*, 1113–1117, doi:10.1289/ehp.9697.

Krotkov, N. A., et al. (2008), Validation of SO_2 retrievals from the Ozone Monitoring Instrument over NE China, *J. Geophys. Res.*, *113*, D16S40, doi:10.1029/2007JD008818.

Lammel, G., Y. S. Ghim, J. A. C. Broekaert, and H.-W. Gao (2006), Heavy metals in air of an eastern China coastal urban area and the Yellow Sea, *Fresenius Environ. Bulletin*, *15*, 1539–1548.

Larsen, I. R. K., and J. E. Baker (2003), Source apportionment of polycyclic aromatic hydrocarbons in the urban atmosphere: A comparison of three methods, *Environ. Sci. Technol.*, *37*, 1873–1881, doi:10.1021/es0206184.

Lee, C. S. L., X.-D. Li, G. Zhang, J. Li, A.-J. Ding, and T. Wang (2007), Heavy metals and Pb isotopic composition of aerosols in urban and suburban areas of Hong Kong and Guangzhou, South China, Evidence of the long-range transport of air contaminants, *Atmos. Environ.*, *41*, 432–447, doi:10.1016/j.atmosenv.2006.07.035.

Lewis, C. W., G. A. Norris, T. L. Conner, and R. C. Henry (2003), Source apportionment of Phoenix $PM_{2.5}$ aerosol with the Unmix receptor model, *J. Air Waste Manage. Assoc.*, *53*, 325–338.

Li, C., L. T. Marufu, R. R. Dickerson, Z. Li, T. Wen, Y. Wang, P. Wang, H. Chen, and J. W. Stehr (2007), In situ measurements of trace gases and aerosol optical properties at a rural site in northern China during EAST-

AIRE IOP 2005, *J. Geophys. Res.*, *112*, D22S04, doi:10.1029/2006JD007592.

Li, J., G. Zhuang, K. Huang, Y. Lin, C. Xu, and S. Yu (2008), Characteristics and sources of air-borne particulate in Urumqi, China, the upstream area of Asia dust, *Atmos. Environ.*, *42*, 776–787, doi:10.1016/j.atmosenv.2007.09.062.

Li, X. L., Y. X. Zhang, M. G. Tan, J. F. Liu, L. M. Bao, G. L. Zhang, Y. Li, and A. Iida (2009), Atmospheric lead pollution in fine particulate matter in Shanghai, China, *J. Environ. Sci.*, *21*, 1118–1124, doi:10.1016/S1001-0742(08)62390-6.

Li, Z., et al. (2007), Preface to special section on East Asian Studies of Tropospheric Aerosols: An International Regional Experiment (EAST-AIRE), *J. Geophys. Res.*, *112*, D22S00, doi:10.1029/2007JD008853.

Lide, D. R. (1998), *CRC Handbook of Chemistry and Physics*, 79th ed., 2496 pp., CRC, Boca Raton, Fla.

Lucey, D., L. Hadjiiski, P. K. Hopke, J. R. Scudlark, and T. Church (2001), Identification of sources of pollutants in precipitation measured at the mid-Atlantic US coast using potential source contribution function (PSCF), *Atmos. Environ.*, *35*, 3979–3986, doi:10.1016/S1352-2310(01)00185-6.

Luke, W. T. (1997), Evaluation of a commercial pulsed fluorescence detector for the measurement of low-level SO_2 concentrations during the Gas-Phase Sulfur Intercomparison Experiment, *J. Geophys. Res.*, *102*, 16,255–16,265, doi:10.1029/96JD03347.

Lv, W., Y. Wang, X. Querol, X. Zhuang, A. Alastuey, A. López, and M. Viana (2006), Geochemical and statistical analysis of trace metals in atmospheric particulates in Wuhan, central China, *Environ. Geol.*, *51*, 121–132, doi:10.1007/s00254-006-0310-5.

Nriagu, J. O., and J. M. Pacyna (1988), Quantitative assessment of world-wide contamination of air, water and soils by trace elements, *Nature*, *333*, 134–139, doi:10.1038/333134a0.

Pacyna, J. M. (1998), Source inventories for atmospheric trace metals, in *Atmospheric Particles, IUPAC Ser. Anal. Phys. Chem. Environ. Syst.*, vol. 5, edited by R. M. Harrison and R. E. Van Grieken, pp. 385–423, John Wiley, Chichester, U. K.

Querol, X., X. Zhuang, A. Alastuey, M. Viana, W. Lv, Y. Wang, A. López, Z. Zhu, H. Wei, and S. Xu (2006), Speciation and sources of atmospheric aerosols in a highly industrialized and emerging mega-city in central China, *J. Environ. Monit.*, *8*, 1049–1059, doi:10.1039/b608768j.

Rahn, K. A. (1981), The Mn/V ratio as a tracer of large-scale sources of pollution aerosol for the Arctic, *Atmos. Environ.*, *15*, 1457–1464, doi:10.1016/0004-6981(81)90352-8.

Shen, X., J. F. Rosen, D. Guo, and S. Wu (1996), Childhood lead poisoning in China, *Sci. Total Environ.*, *181*, 101–109, doi:10.1016/0048-9697(95)04956-8.

Shen, X., S. Wu, and C. Yan (2001), Impacts of low-level lead exposure on development of children: Recent studies in China, *Clin. Chim. Acta*, *313*, 217–220, doi:10.1016/S0009-8981(01)00675-1.

Shen, Z. X., J. J. Cao, R. Arimoto, R. J. Zhang, D. M. Jie, S. X. Liu, and C. S. Zhu (2007), Chemical composition and source characterization of spring aerosol over Horqin sand land in northeastern China, *J. Geophys. Res.*, *112*, D14315, doi:10.1029/2006JD007991.

Streets, D. G., et al. (2003), An inventory of gaseous and primary aerosol emissions in Asia in the year 2000, *J. Geophys. Res.*, *108*(D21), 8809, doi:10.1029/2002JD003093.

Sun, Y., G. Zhuang, Y. Wang, L. Han, J. Guo, M. Dan, W. Zhang, Z. Wang, and Z. Hao (2004), The air-borne particulate pollution in Beijing—Concentration, composition, distribution and sources, *Atmos. Environ.*, *38*, 5991–6004, doi:10.1016/j.atmosenv.2004.07.009.

Sun, Y., G. Zhuang, Y. Wang, X. Zhao, J. Li, Z. Wang, and Z. An (2005), Chemical composition of dust storms in Beijing and implications for the mixing of mineral aerosol with pollution aerosol on the pathway, *J. Geophys. Res.*, *110*, D24209, doi:10.1029/2005JD006054.

Sun, Y., G. Zhuang, W. Zhang, Y. Wang, and Y. Zhuang (2006), Characteristics and sources of lead pollution after phasing out leaded gasoline in Beijing, *Atmos. Environ.*, *40*, 2973–2985, doi:10.1016/j.atmosenv.2005.12.032.

Sun, Y., et al. (2010), Asian dust over northern China and its impact on the downstream aerosol chemistry in 2004, *J. Geophys. Res.*, *115*, D00K09, doi:10.1029/2009JD012757.

Thornton, J. A., et al. (2010), A large atomic chlorine source inferred from mid-continental reactive nitrogen chemistry, *Nature*, *464*, 271–274, doi:10.1038/nature08905.

U.S. Environmental Protection Agency (U.S. EPA) (2006), Air quality criteria for lead, vol. 1, *EPA/600/R-05/144aF*, Research Triangle Park, N. C.

U.S. Environmental Protection Agency (U.S. EPA) (2007a), Review of the national ambient air quality standards for lead: Policy assessment of scientific and technical information, *EPA-452/R-07–013*, Research Triangle Park, N. C.

U.S. Environmental Protection Agency (U.S. EPA) (2007b), EPA Unmix 6.0 fundamentals and user guide, *EPA-600/R-07–089*, Research Triangle Park, N. C.

Wang, S., and J. Zhang (2006), Blood lead levels in children, *China, Environ. Res.*, *101*, 412–418, doi:10.1016/j.envres.2005.11.007.

Wang, W., X. Liu, L. Zhao, D. Guo, X. Tian, and F. Adams (2006), Effectiveness of leaded petrol phase-out in Tianjin, China, based on the aerosol lead concentration and isotope abundance ratio, *Sci. Total Environ.*, *364*, 175–187, doi:10.1016/j.scitotenv.2005.07.002.

Wang, X., X. Bi, G. Sheng, and J. Fu (2006), Chemical composition and sources of PM_{10} and $PM_{2.5}$ aerosols in Guangzhou, China, *Environ. Monit. Assess.*, *119*, 425–439, doi:10.1007/s10661-005-9034-3.

Wang, Y., G. Zhuang, A. Tang, H. Yuan, Y. Sun, S. Chen, and A. Zheng (2005), The ion chemistry and source of $PM_{2.5}$ aerosol in Beijing, *Atmos. Environ.*, *39*, 3771–3784, doi:10.1016/j.atmosenv.2005.03.013.

Wang, Y., G. Zhuang, A. Tang, W. Zhang, Y. Sun, Z. Wang, and Z. An (2007), The evolution of chemical components of aerosols at five monitoring sites of China during dust storms, *Atmos. Environ.*, *41*, 1091–1106, doi:10.1016/j.atmosenv.2006.09.015.

Xu, H., Y. Wang, T. Wen, and X. He (2007a), Size distributions and vertical distributions of water soluble ions of atmospheric aerosol in Beijing (in Chinese), *Environ. Sci.*, *28*, 14–19.

Xu, H., Y. Wang, T. Wen, and X. He (2007b), Size distributions and vertical distributions of metal elements of atmospheric aerosol in Beijing (in Chinese), *Environ. Chem.*, *26*, 675–679.

Xuan, J. (2005), Emission inventory of eight elements, Fe, Al, K, Mg, Mn, Na, Ca, and Ti, in dust source region of East Asia, *Atmos. Environ.*, *39*, 813–821, doi:10.1016/j.atmosenv.2004.10.029.

Yang, Y., Y. Wang, T. Wen, W. Li, Y. Zhao, and L. Liang (2009), Elemental composition of $PM_{2.5}$ and PM_{10} at Mount Gongga in China during 2006, *Atmos. Res.*, *93*, 801–810, doi:10.1016/j.atmosres.2009.03.014.

Ye, B., X. Ji, H. Yang, X. Yao, C. K. Chan, S. H. Cadle, T. Chan, and P. A. Mulawa (2003), Concentrations and chemical composition of $PM_{2.5}$ in Shanghai for a 1-year period, *Atmos. Environ.*, *37*, 499–510, doi:10.1016/S1352-2310(02)00918-4.

Zhang, Q., et al. (2009), Asian emissions in 2006 for the NASA INTEX-B mission, *Atmos. Chem. Phys.*, *9*, 5131–5153, doi:10.5194/acp-9-5131-2009.

Zhang, X. Y., S. L. Gong, Z. X. Shen, F. M. Mei, X. X. Xi, L. C. Liu, Z. J. Zhou, D. Wang, Y. Q. Wang, and Y. Cheng (2003a), Characterization of soil dust aerosol in China and its transport and distribution during 2001 ACE-Asia: 1. Network observations, *J. Geophys. Res.*, *108*(D9), 4261, doi:10.1029/2002JD002632.

Zhang, X. Y., S. L. Gong, R. Arimoto, Z. X. Shen, F. M. Mei, D. Wang, and Y. Cheng (2003b), Characterization and temporal variation of Asian dust aerosol from a site in the northern China deserts, *J. Atmos. Chem.*, *44*, 241–257, doi:10.1023/A:1022900220357.

Zhang, X. Y., Y. Q. Wang, D. Wang, S. L. Gong, R. Arimoto, L. J. Mao, and J. Li (2005), Characterization and sources of regional-scale transported carbonaceous and dust aerosols from different pathways in coastal and sandy land areas of China, *J. Geophys. Res.*, *110*, D15301, doi:10.1029/2004JD005457.

Zhang, X., G. Zhuang, J. Guo, K. Yin, and P. Zhang (2007), Characterization of aerosol over the Northern South China Sea during two cruises in 2003, *Atmos. Environ.*, *41*, 7821–7836, doi:10.1016/j.atmosenv.2007.06.031.

Zhang, Y. P., X. F. Wang, H. Chen, X. Yang, J. M. Chen, and J. O. Allen (2009), Source apportionment of lead-containing aerosol particles in Shanghai using single particle mass spectrometry, *Chemosphere*, *74*, 501–507, doi:10.1016/j.chemosphere.2008.10.004.

R. R. Dickerson, Department of Atmospheric and Oceanic Science, University of Maryland, College Park, MD 20742, USA.

C. Li and Z. Li, Earth System Science Interdisciplinary Center, University of Maryland, College Park, MD 20742, USA. (can.li@nasa.gov)

S.-C. Tsay, NASA Goddard Space Flight Center, Greenbelt, MD 20771, USA.

Y. Wang, T. Wen, and Y. Zhao, Institute of Atmospheric Physics, Chinese Academy of Sciences, Beijing 100029, China.

Y. Yang, National Research Center for Environmental Analysis and Measurement, Beijing 100029, China.